Front. Optoelectron. 2014, 7(1): 59–63
DOI 10.1007/s12200-013-0363-5

RESEARCH ARTICLE

A micro-spectrometer with phase modulation array

Tao YANG[1], Yuchao CHEN[1], Xing'ao LI[1], Wei HUANG (✉)[1], Yongyuan ZHU (✉)[2]

1 Key Laboratory for Organic Electronics & Information Displays, Nanjing University of Posts and Telecommunications, Nanjing 210023, China
2 National Laboratory of Solid State Microstructures, Nanjing University, Nanjing 210093, China

Abstract A micro-spectrometer with phase modulation array is investigated in this paper. The vital component of this micro-spectrometer is a micro-interferometer array, which is built on a charge-coupled device (CCD) or a complementary metal oxide semiconductor (CMOS). Each element of micro-interferometer array is formed by polymethyl methacrylate (PMMA) grooves with different depth. When we illuminate the surface of the interferometer array, different interference intensity distribution would be formed at the bottom of each micro-interferometer. Optical power of this interferometer can be measured by the pixels of CCD or CMOS. The data can be substituted into a linear system. By solving the linear system with Tikhonov regularization method, spectrum of the incident beam can be reconstructed. Simulation results prove that the detection range of the spectrometer is a wide wavelength range covering from 300 to 1100 nm. Furthermore, the wavelength resolution of the device reaches picometer level. In comparison with conventional spectrometers, the novel spectrometer has distinct advantages of small size, low cost, high resolution, wide spectral measurement range, real-time measurement, and so on.

Keywords micro-spectrometer, spectrum reconstruction, Tikhonov regularization

1 Introduction

Spectrometers are a sort of optical instruments used to analyze the composition or content of samples by detecting their spectral information [1,2]. They are widely applied in various fields, such as astronomy, biology, chymistry, agriculture, metallurgy and geology, and so on [3–5]. However, current Fourier transform spectrometers, particularly those using the scanning mirror mechanisms, are quite bulky. Furthermore, they use fast Fourier transform (FFT) method to reconstruct the incident spectrum, Therefore, Fourier transform spectrometers only can be used in the infrared range [6–8].

With the development of computer technology and micro-fabrication process, some miniature spectrometers are designed to meet the requirements in wide fields. Some miniature spectrometers using micro-electro-mechanical systems (MEMS), micro-opto-electro-mechanical systems (MOEMS), integrated optics technology and binary optics technology have been reported in literatures [9–11]. For example, a Fabry-Perot (F-P) based miniature spectrometer with compact size has been developed, which can realize static broadband measurement. However, because the F-P cavity in the miniature device is usually based on a first-order mode operation, the thickness of mirror metal layer limits the spectral resolution of the device. Although higher order mode operation can improve the resolution, it is difficult to guarantee two mirrors in the device are fully parallel. Therefore, the resolution of the spectrometer cannot be very high [12,13].

To overcome limitations of the above spectrometers, we proposed a micro-spectrometer with phase modulation array. Many phase modulation grooves are adopted to form a micro-interferometer-dimensional array, which can be used to modulate the phase of the incident light to achieve static measurement rather than changing the position of movable mirror as in traditional Fourier transform spectrometers. The proposed spectrometer has the advantages of small size, low cost, high resolution, and wide spectral measurement range. Furthermore, it can realize fast measurement as well.

2 Operation principle of spectrometer

As shown in Fig. 1, the core element of the spectrometer is a two-dimensional (2D) array of micro-interferometer built on a polymethyl methacrylate (PMMA) substrate. Each micro-interferometer is formed by two PMMA grooves as

Received July 18, 2013; accepted October 22, 2013

E-mail: wei-huang@njut.edu.cn, yyzhu@nju.edu.cn, burak0320@foxmail.com

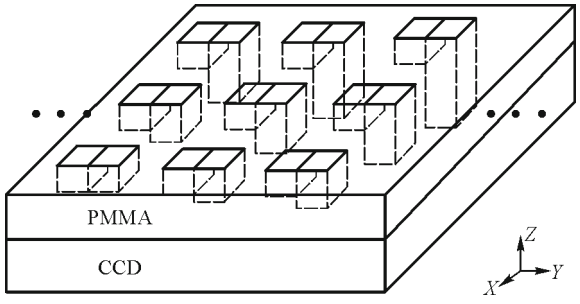

Fig. 1 Schematic of optical spectrometer

a basic structural unit. The depths of these two grooves are different from each other. The detector array chip is arranged under the PAMA substrate, which could be either charge-coupled device (CCD) or complementary metal oxide semiconductor (CMOS). In case of crosstalk of different micro-interferometers, we keep certain space among micro-interferometers. The detector array provides a light shielding plate. And there are a series of same apertures below the interferometers.

We enlarge the cross section of an interferometer element to demonstrate the operation principle of the device. As shown in Fig. 2, two confocal lens with a pin hole are placed above the interferometer array to ensure the direction of the incident light is perpendicular to the surface of the array. When a incident light arrives from the top of a interferometer, the incident light is divided into two parts by the two phase grooves of the interferometer. Since the two phase grooves are of different depths, there exists a phase delay between the two beam portions. When the two beam portions meet up again at the detector surface, interference occurs and the interference intensity is recorded.

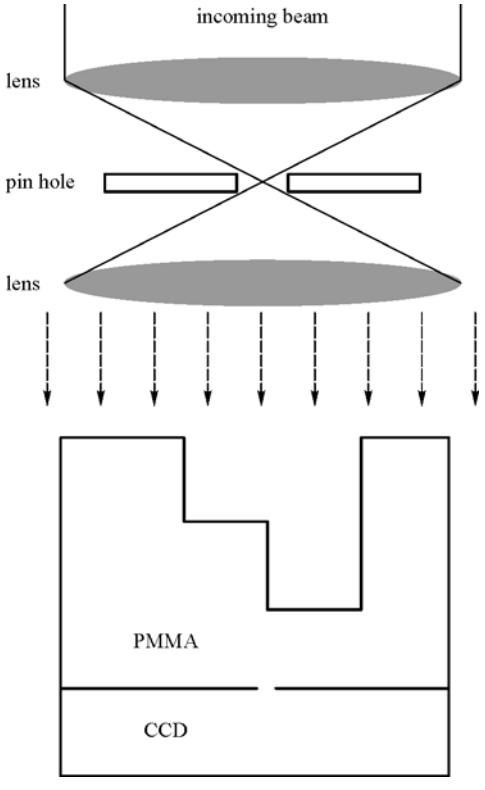

Fig. 2 Cross-section of interferometer element

The groove depth is designed to be unique so that all the interferometer elements will provide different phase delays. Since each frequency component in the incident beam corresponds to a unique phase difference of the two beam portions, the total intensity received by each pixel, which is resulted from the addition of the interference signals from all the frequency components in the beam, should also be unique. This also means that the distribution of the detected intensities by the pixels is governed by the spectral content of the incident beam, and recovery of spectral information should be possible.

As shown in Fig. 3, the incoming beam is uniformly divided into n frequency components $f_1,f_2,...,f_n$ with Δf, the total power of the incoming beam can be approximately calculated by using the theory of integral calculus when n is large enough, i.e.,

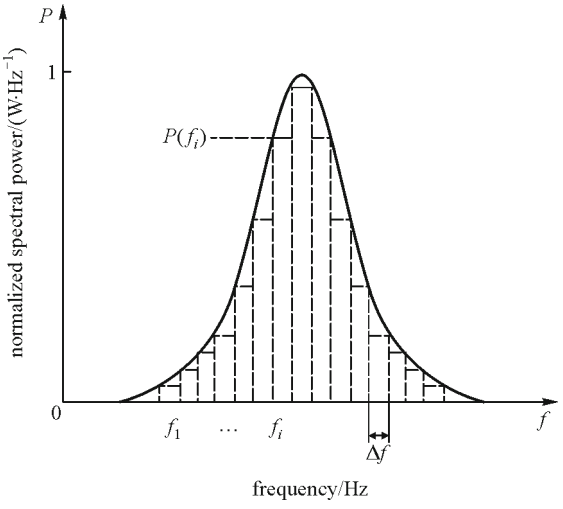

Fig. 3 Division of source spectrum

$$P_0 = P(f_1)\Delta f + P(f_2)\Delta f + \cdots + P(f_n)\Delta f, \quad (1)$$

where $P(f_n)$ (n = 1,2,…,N) is the power of frequency component f_n (n = 1,2,…,N). After passing through the holes array, the beam can be detected by a series of CCD pixels. The power measured by one of the pixels is given by

$$P = C_1P(f_1)\Delta f + C_2P(f_2)\Delta f + \cdots + C_nP(f_n)\Delta f, \quad (2)$$

where C_{xn} (n = 1,2,…,N) is the detection coefficient of the frequency, f_n, for the xth pixel. The detection coefficient is the ratio of the power obtained by the CCD pixel to the power of the incident beam for frequency f_n, which is

constant and measurable.

If N interferometers are illuminated by the incoming beam, a 2D map of optical intensities can be measured by the CCD pixels. At the same time, the intensities can be represented by the following equations:

$$\begin{aligned} P_1 &= C_{11}P(f_1)\Delta f + C_{12}P(f_2)\Delta f + \cdots + C_{1n}P(f_n)\Delta f, \\ P_2 &= C_{21}P(f_1)\Delta f + C_{22}P(f_2)\Delta f + \cdots + C_{2n}P(f_n)\Delta f, \\ &\cdots \\ P_n &= C_{n1}P(f_1)\Delta f + C_{n2}P(f_2)\Delta f + \cdots + C_{nn}P(f_n)\Delta f, \end{aligned} \quad (3)$$

where C_{ij} ($i=$ 1,2,...,n, $j=$ 1,2,...,n) is the detection coefficient of frequency f_j for the ith pixel. Therefore, once we know the detection coefficients and the detected intensities from different pixels, i.e.,

$$\boldsymbol{C} = \begin{pmatrix} C_{11} & C_{12} & \cdots & C_{1n} \\ C_{21} & C_{22} & \cdots & C_{2n} \\ \vdots & \vdots & \ddots & \vdots \\ C_{n1} & C_{n2} & \cdots & C_{nn} \end{pmatrix}, \boldsymbol{y} = \begin{pmatrix} P_1 \\ P_2 \\ \vdots \\ P_n \end{pmatrix}, \quad (4)$$

we can get a system of linear equations

$$\boldsymbol{Cx} = \boldsymbol{y}, \quad (5)$$

where

$$\boldsymbol{x} = \begin{pmatrix} P(f_1)\cdot\Delta f \\ P(f_2)\cdot\Delta f \\ \vdots \\ P(f_n)\cdot\Delta f \end{pmatrix}. \quad (6)$$

Consequently, the spectrum of incoming beam can be obtained by fitting $P(f_1)$, $P(f_2)$,...,$P(f_n)$, which are the elements of the matrix

$$\tilde{\boldsymbol{x}} = \boldsymbol{x}/\Delta f = \begin{pmatrix} P(f_1) \\ P(f_2) \\ \vdots \\ P(f_n) \end{pmatrix}. \quad (7)$$

Therefore, we can obtain the incident spectrum by fitting the corresponding power $P(f_i)$ of each frequency components. However, the data error of matrix $\boldsymbol{C}$ and $\boldsymbol{y}$ due to the unavoidable measurement noises makes this linear system become an ill-posed problem. It is difficult to solve such a large system of linear equations by using ordinary nonstationary iterative methods due to instability problems. Named after Andrei Nikolaevich Tikhonov, the Tikhonov regularization approach [14–16] has been shown to be effective in solving ill-posed problems. The reconstruction procedure costs about one second by using Tikhonov regularization method with MATLAB programs, which indicates the feasibility of real-time measurement for many applications.

3 Simulation results

3.1 High-resolution spectral recovery

We have performed a series of 2D simulation experiments by varying the depth of one groove from 0 to 10 μm, as demonstrated in Fig. 4. Finite-difference time-domain (FDTD) solutions are used to study the interferometer structure. To smooth out edge effects, we use a transverse electric (TE) mode plane wave source acting as total-field scattered-field (TFSF) source with perfectly matched layer (PML) boundaries around. There is only one interferometer inside the PML boundaries, which goes through the PMMA layer in the direction normal to the source light propagation. The values in matrix $\boldsymbol{C}$ and $\boldsymbol{y}$ can be obtained from a frequency domain power monitor by a series of simulation experiments and the initial data can be processed using Matlab.

As shown in Fig. 4, the solid line is original spectrum, and dotted line is the recovery one. It can be seen from Fig. 4 that, the solid and dotted lines are almost overlapped, which means that recovery spectrum has no obvious distortion. But it can be seen in the enlarged diagram that the recovery spectrum has some differences from the original one. Figure 4(a) shows that 100 frequency components are reconstructed in the range from 400 to 800 THz. The resolution is 4 THz in terms of frequency, which refers to 1.88 nm in wavelength. Figure 4(b) shows that 200 frequency components are reconstructed in the range from 400 to 800 THz, and the resolution is 2 THz, which is equivalent to 939.2 pm in wavelength.

If we divide a large number of copies, the spectral recovery range will be smaller, we can achieve spectral recovery with higher resolution. Figure 5 shows that 200 frequency components are reconstructed in the range from 747.61 to 749.8 THz. The resolution is 9.35 GHz in terms of frequency, which refers to 4.98 pm in wavelength. If we narrow the range of recovery wavelength and increase divided copies n, we can also further improve the resolution. Therefore it is suggested that the wavelength resolution of the spectrometer can be reached picometer scale to meet most of actual requirements.

3.2 Wide spectral recovery range

The spectrometer can also be used to perform a wide spectral range of spectral recovery. The range of spectral detection in actual device is mainly determined by the spectral response range of the using detector. Ordinary CCD can detect light from ultraviolet (UV) to near infrared (IR), the wavelength range from 300 to 1100 nm, which

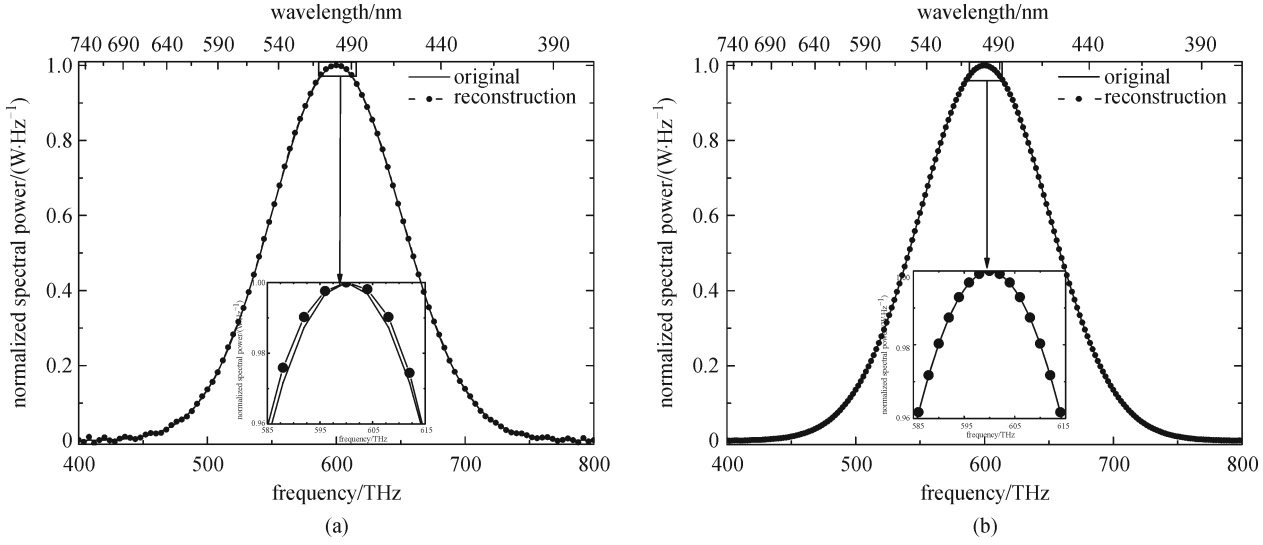

Fig. 4 Spectrum reconstruction with different n. (a) n = 100; (b) n = 200

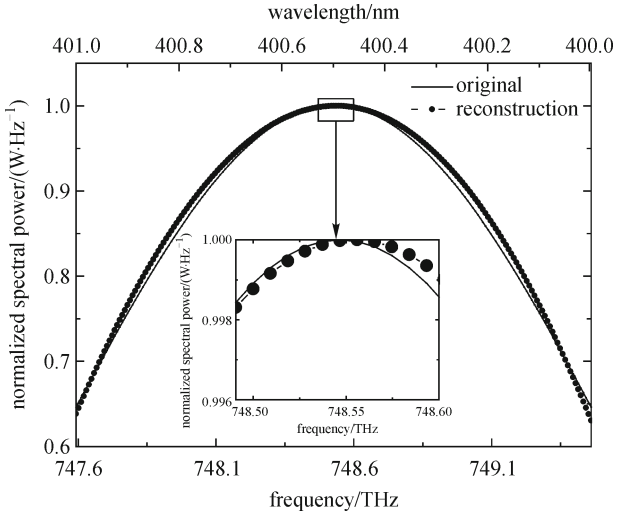

Fig. 5 Spectrum reconstruction with high spectral resolution

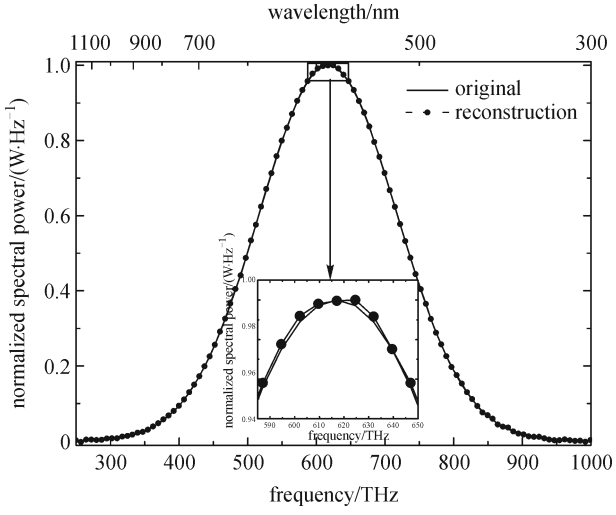

Fig. 6 Reconstruction spectrum in the range from UV to IR

corresponds to the frequency range from 273 to 1000 THz, the simulation results in the range from UV to IR is shown in Fig. 6.

3.3 Spectrum of complex waveform recovery

The results given above are assuming that the incident light is Gaussian spectrum, but actually the spectral shape of the incident light is often complex and irregular. For example, in geological exploration, detected target is mixed substance, and it requires the spectrometer with sufficient resolution to distinguish the different elements by characteristic spectrum. Figure 7 shows the result of a complex spectrum recovery, the frequency of spectral recovery ranged from 400 to 800 THz, the frequency resolution is 2 THz and the highest wavelength resolution is 0.94 nm.

3.4 Factors affecting spectrum reconstruction

We also analyze the impact factors for satisfactory reconstructions, which include: the sensitivity of the CCD, the signal-to-noise ratio (SNR) of the CCD, size and material of the spectrometer components, precision of fabrication technology. One may raise a question, i.e., whether is there a limit for each impact factor? In other word, whether does obvious distortion occur if an impact factor exceeds a limit? However, simulation results have shown that these factors are not isolated from each other. It is nearly impossible to state a range for the value of one factor because a satisfactory reconstruction depends on many parameters. To avoid obvious distortion and obtain

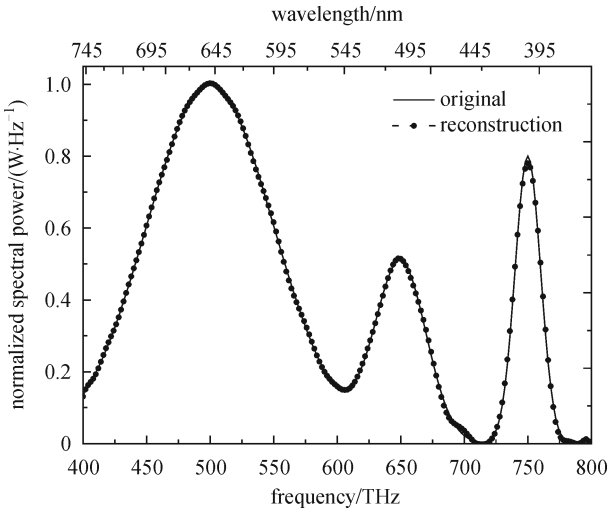

Fig. 7 Reconstruction of complex spectrum

satisfactory results, two rules must be satisfied:

1) The peak width of original spectrum should be at least larger than the reconstruction resolution. The resolution can be calculated by the spectrum range over the number of the frequency division. If the peak width is too narrow, it is too difficult to make the reconstruction curve smooth and continuous with Tikhonov regularization method and obvious distortion may occur.

2) The CCD pixels can separate the difference of two close interferometers. It is possible that two interferometers are different, but we get the same power from the CCD pixels with the two interferometers due to the poor SNR of CCD or small variation of step height or other reasons. If the CCD pixels obtain the same value from two expected different interferometers, it is difficult to solve the corresponding linear system hence obvious distortion may occur.

4 Conclusions

We have proposed a novel micro-spectrometer using a groove array, which is demonstrated by using FDTD simulations. The spectrometer relies on advanced nano technology and micro-electro-mechanical system. The proposed device is low-cost and easy to be fabricated for its simple structure. It can be used in complex environment measurements due to its static configuration. The proposed design takes advantage of the well-established CCD and precision moulding technologies to produce miniature, low-cost and high performance optical spectrometers, which may find applications in a wide range of areas.

Acknowledgements This work was supported by the National Natural Science Foundation of China (Grant Nos. 6110611, 51172110, 651372119 and 61377019), the National Basic Research Program of China (Nos. 2012CB933301 and 2009CB930600), the Research Fund of National Laboratory of Solid State Microstructure (No. M25008).

References

1. McCain S T, Gehm M E, Wang Y, Pitsianis N P, Brady D J. Coded aperture Raman spectroscopy for quantitative measurements of ethanol in a tissue phantom. Society for Applied Spectroscopy, 2006, 60(6): 663–671
2. Gehm M E, John R, Brady D J, Willett R M, Schulz T J. Single-shot compressive spectral imaging with a dual-disperser architecture. Optics Express, 2007, 15(21): 14013–14027
3. Zhang C M, Jian X H. Wide-spectrum reconstruction method for a birefringence interference imaging spectrometer. Optics Letters, 2010, 35(3): 366–368
4. Schliesser A, Brehm M, Keilmann F, van der Weide D. Frequency-comb infrared spectrometer for rapid, remote chemical sensing. Optics Express, 2005, 13(22): 9029–9038
5. Shogenji R, Kitamura Y, Yamada K, Miyatake S, Tanida J. Multispectral imaging using compact compound optics. Optics Express, 2004, 12(8): 1643–1655
6. Ataman C, Urey H. Compact Fourier transform spectrometers using FR4 platform. Sensors and Actuators. A, Physical, 2009, 151(1): 9–16
7. Ataman C, Urey H, Wolter A. A Fourier transform spectrometer using resonant vertical comb actuators. Journal of Micromechanics and Microengineering, 2006, 16(12): 2517–2523
8. Knipp D, Stiebig H, Bhalotra S R, Bunte E, Kung H L, Miller D A B. Silicon-based micro-Fourier spectrometer. IEEE Transactions on Electron Devices, 2005, 52(3): 419–426
9. Wang S W, Chen X, Lu W, Wang L, Wu Y, Wang Z. Integrated optical filter arrays fabricated by using the combinatorial etching technique. Optics Letters, 2006, 31(3): 332–334
10. Wang S W, Xia C, Chen X, Lu W, Li M, Wang H, Zheng W, Zhang T. Concept of a high-resolution miniature spectrometer using an integrated filter array. Optics Letters, 2007, 32(6): 632–634
11. Oka K, Kato T. Spectroscopic polarimetry with a channeled spectrum. Optics Letters, 1999, 24(21): 1475–1477
12. Wolffenbuttel R F. State-of-the-art in integrated optical micro-spectrometers. IEEE Transactions on Instrumentation and Measurement, 2004, 53(1): 197–202
13. Marinelli W J, Gittins C M, Gelb A H, Green B D. Tunable Fabry-Perot ealon-based long-wavelength infrared imaging spectroradiometer. Applied Optics, 1999, 38(12): 2594–2604
14. Honerkamp J, Weese J. Tikhonov regularization method for ill-posed problems. Continuum Mechanics and Thermodynamics, 1990, 2(1): 17–30
15. Wu L M. A parameter choice method for Tikhonov regularization. Electronic Transactions on Numerical Analysis, 2003, 16: 107–128
16. Wang Z W, Liu J. New model function methods for determining regularization parameters in linear inverse problems. Applied Numerical Mathematics, 2009, 59(10): 2489–2506